Optimal Dispatch for Battery Energy Storage Station in Distribution Network Considering Voltage Distribution Improvement and Peak Load Shifting

Xiangjun Li, *Senior Member*, *IEEE*, Rui Ma, Wei Gan, and Shijie Yan

***Abstract*—Distribution networks are commonly used to demonstrate low-voltage problems. A new method to improve voltage quality is using battery energy storage stations (BESSs), which has a four-quadrant regulating capacity. In this paper, an optimal dispatching model of a distributed BESS considering peak load shifting is proposed to improve the voltage distribution in a distribution network. The objective function is to minimize the power exchange cost between the distribution network and the transmission network and the penalty cost of the voltage deviation. In the process, various constraints are considered, including the node power balance, single/two-way power flow, peak load shifting, line capacity, voltage deviation, photovoltaic station operation, main transformer capacity, and power factor of the distribution network. The big *M* method is used to linearize the nonlinear variables in the objective function and constraints, and the model is transformed into a mixed-integer linear programming problem, which significantly improves the model accuracy. Simulations are performed using the modified IEEE 33-node system. A typical time period is selected to analyze the node voltage variation, and the results show that the maximum voltage deviation can be reduced from 14.06% to 4.54%. The maximum peak-valley difference of the system can be reduced from 8.83 to 4.23 MW, and the voltage qualification rate can be significantly improved. Moreover, the validity of the proposed model is verified through simulations.**

***Index Terms*—Energy storage station, distribution network voltage regulation, peak load shifting, mixed integer programming.**

I. Introduction

THE development of renewable energy has attracted increasing attention for global energy transformation [1], [2] owing to the increasingly serious environmental issues caused by the use of conventional energy sources. Distributed generation (DG) is an important feature in the future development of power grids [3]. As an important part of a power grid, the distribution network is close to power users and closely related to their daily lives. DG unquestionably affects the existing distribution network to a certain extent.

Coordination and interaction between DG and distribution networks is necessary to ensure the comprehensive utilization of resources and energy, energy interconnection, and improvement of power quality [4], [5]. However, the power generation characteristics of DG are significantly influenced by factors such as season and weather owing to its intermittent and fluctuating nature [6] - [8]. The distribution network has switched from the traditional single-power-source radial network to a multi-power-source complex network as a result of the increasing penetration of DG in the distribution network [9], [10]. The traditional distribution network is faced with several problems such as high voltage drops [11] - [13], renewable energy accommodation [14]-[17], and difficulties in network expansion [18]-[20].

A battery energy storage station (BESS) has the advantages of quick response, reduced pollution, small space requirement, and a short construction period [21], [22]. It can be used to relieve power supply shortage during peak periods and to provide peak shaving and valley filling services for the system [23], [24]. It can also address the issue of power shortage caused by insufficient reactive power compensation by outputing reactive power, providing voltage regulation service for the system, improving the voltage of the terminal power network [25], and postponing expansion of transmission capacity [26]. In China, the main owner of grid-side BESSs is the State Grid Corporation of China. The BESSs can be directly controlled by the system operator during scheduling or control processes. China is trying to improve the market and price mechanism of power auxiliary services, including frequency modulation with BESSs, peak regulation, backup power supply, black start, demand-side re-

Manuscript received: March 23, 2020; revised: July 20, 2020; accepted: August 3, 2020. Date of CrossCheck: August 3, 2020. Date of online publication: October 6, 2020.

This work was supported by the Science and Technology Project of State Grid Corporation of China "Intelligent Coordination Control and Energy Optimization Management of Super-large Scale Battery Energy Storage Power Station Based on Information Physics Fusion – Simulation Model and Transient Characteristics of Super-large Scale Battery Energy Storage Power Station" (No. DG71-18-009).

X. Li (corresponding author), R. Ma, and W. Gan are with the State Key Laboratory of Control and Operation of Renewable Energy and Storage Systems, China Electric Power Research Institute, Beijing, China (e-mail: li_xiangjun@126.com; merry0111@163.com; weigan@hust.edu.cn).

S. Yan is with the College of Information and Engineering, Northeastern University, Shenyang, China (e-mail: yanshijie@mail.neu.edu.cn).

DOI: 10.35833/MPCE.2020.000183

sponse, and other auxiliary services, which fully reflect the market value of BESS.

In some studies, the advantages of BESSs have been investigated in terms of improved voltage quality in the distribution network [21], [22], [25]. Distributed and localized control methods have also been proposed for distributed BESSs [27]. Distributed control with a consensus algorithm keeps the feeder voltage in the required range within the desired range of the state of charge. The entire control structure makes good use of the capacity of BESSs under various operation conditions while ensuring voltage regulation. In [28], a heuristic strategy was proposed based on voltage sensitivity analysis to select the most effective location to install a certain number of BESSs in the network while avoiding the combinatorial nature of the problem. Moreover, in [29], a voltage control scheme suitable for installing BESSs in a low-voltage distribution network was proposed. The basic feature of this approach is that the minimal information is required to predict potential voltage problems and determine the BESS control strategy, which enables the elimination of these potential problems in advance. Another study [30] proposed a concept to solve the voltage fluctuation problem in a distribution network with high penetration of photovoltaic (PV) system and BESSs. In [31], a coordination method of multi-battery energy storage systems was proposed to solve the low-voltage problem in a distribution network. In [32], a virtual energy storage system was investigated, which provides voltage control in a distribution network to accommodate more DG systems.

The contributions of this study are twofold. First, an optimal dispatch model for distributed energy storage is proposed to optimize the operation of the distribution network, which includes the voltage distribution improvement and peak load shifting. The power exchange cost of the distribution and transmission networks and the minimum penalty cost of voltage deviation are considered as the objective functions. Various constraints such as voltage limits, power flow, and line capacity, are considered. Second, mixed-integer linear programming (MILP) is applied, which avoids random initialization and repeated iterations and improves the accuracy of the model. This model can fully utilize the regulating capacity of the BESS, which plays a significant role in voltage regulation, load shifting, and renewable energy consumption. In addition, optimal operation contributes to postponing the construction of transmission lines and increasing the transformer capacity, thereby significantly reducing the system costs. The effectiveness of the proposed optimal dispatch model is verified using an example.

II. Optimal Dispatch Model of Distributed Energy Storage

A. Objective Function

The aim of the established optimal dispatch model of the distributed energy storage in the distribution network is to minimize the power exchange cost between the distribution network and the transmission network and the penalty cost of node voltage deviation, as shown in (1).

$$\min F = \sum_{t=1}^{T} C_t P_t + \rho \sum_{i}^{N} \sum_{t}^{T} |U_{i,t} - 1| \tag{1}$$

where F is the objective function; ρ is the penalty coefficient of the voltage deviation, which should be adjusted according to the operation of the distribution network; T is the total number of time periods for scheduling the distribution; N is the total number of nodes in the distribution network; P_t is the interactive power between the distribution network and the transmission network at time period t; C_t is the time-of-use price of power supply for the distribution network system; and $U_{i,t}$ is the voltage amplitude of node i in the distribution network at time period t.

B. Constraints

The constraints of the proposed model include the power balance constraints of system nodes, the power flow constraints of distribution network, the operation constraints of BESSs, the peak load shifting constraints of distribution networks, the transmission capacity constraints of line, the voltage constraints of system nodes, the operation constraints of PV power station, and the main transformer capacity and power factor constraints of distribution network.

1) Power Balance Constraints of System Node

Each node in the system needs to maintain a power balance in both active power and reactive power. As shown in Fig. 1, for any node i at time period t, the active power balance constraint should satisfy (2). Similarly, the reactive power balance constraint of node should satisfy (3).

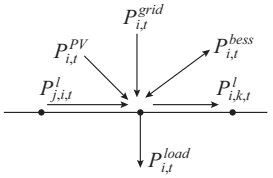

Fig. 1. Diagram of power flow direction of node.

$$\sum_{j,i\in\Phi_l} P_{j,i,t}^{l} - \sum_{i,k\in\Phi_l} P_{i,k,t}^{l} + P_{i,t}^{grid} + P_{i,t}^{pv} + P_{i,t}^{bess} = P_{i,t}^{load} \tag{2}$$

$$\sum_{j,i\in\Phi_l} Q_{j,i,t}^{l} - \sum_{i,k\in\Phi_l} Q_{i,k,t}^{l} + Q_{i,t}^{grid} + Q_{i,t}^{pv} + Q_{i,t}^{bess} = Q_{i,t}^{load} \tag{3}$$

where $P_{j,i,t}^{l}$ and $Q_{j,i,t}^{l}$ are the injected active and reactive power of the line connected with node i, respectively; $P_{i,k,t}^{l}$ and $Q_{i,k,t}^{l}$ are the output active and reactive power of the line connected with node i, respectively; $P_{i,t}^{grid}$ and $Q_{i,t}^{grid}$ are the active and reactive power injected into node i by the power grid, respectively; $P_{i,t}^{pv}$ and $Q_{i,t}^{pv}$ are the active and reactive power injected into node i by the PV power station, respectively; $P_{i,t}^{bess}$ and $Q_{i,t}^{bess}$ are the injected or output active and reactive power of the BESS, respectively; $P_{i,t}^{load}$ and $Q_{i,t}^{load}$ are the active and reactive power of the load, respectively; and Φ_l is the set of all lines in the system.

2) Power Flow Constraint of Distribution Network with Distributed Energy Storage

A backward/forward sweep load flow algorithm [33], [34] is commonly used in the power flow calculation of a distribution network. To analyze the distributed energy storage

and solve the problem of voltage adjustment in the distribution network using a mathematical programming algorithm, a simplified power flow model is formulated on the basis of this algorithm. The longitudinal voltage drop is significantly larger than the transverse voltage drop because the distribution network is an inductive network. Hence, the transverse component of the voltage is ignored. Moreover, the traditional unidirectional power flow in the power grid is not applicable because of the distributed power supply and energy storage. Therefore, in this study, the unidirectional/bidirectional constraint conditions of power flow in the distribution network are established. In the calculation process, the bidirectional power flow constraint can be adjusted according to the actual grid structure and the operation state of the grid.

The single/bidirectional constraint of power flow in a distribution network containing distributed energy storage is described in (4) and (5).

$$\frac{r_{j,i}^{l}P_{j,i,t}^{l}+x_{j,i}^{l}Q_{j,i,t}^{l}}{U_0}=(2D_{j,i,t}^{l}-1)(U_{j,t}-U_{i,t}) \tag{4}$$

$$\begin{cases}P_{j,i,t}^{l}D_{j,i,t}^{l}\geq 0\\ P_{j,i,t}^{l}(1-D_{j,i,t}^{l})\leq 0\end{cases} \tag{5}$$

where $r_{j,i}^{l}$ and $x_{j,i}^{l}$ are the resistance and reactance of line l, respectively; $U_{i,t}$ and $U_{j,t}$ are the voltages at the beginning node i and the end node j at time period t, respectively; U_0 is the voltage of the balance node of the distribution network; and $D_{j,i,t}^{l}$ is a binary variable representing the direction of the power flow, whose value is 1 if the line power flow is consistent with the predefined branch direction or 0 otherwise.

Equation (4) is the constraint of the line voltage drop, and (5) represents the relationship between the $P_{j,i,t}^{l}$ and the binary variable $D_{j,i,t}^{l}$. If the value of $D_{j,i,t}^{l}$ is 1, (5) makes $P_{j,i,t}^{l}\geq 0$, and the power flow direction is from j to i. If the value of $D_{j,i,t}^{l}$ is 0, (5) makes $P_{j,i,t}^{l}\leq 0$, and the power flow direction is from i to j.

3) Operation Constraints of BESS

The BESS model established in this study has a four-quadrant regulating capacity, as shown in Fig. 2.

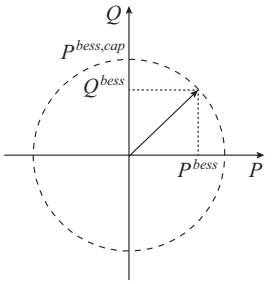

Fig. 2. Diagram of four-quadrant regulating capacity of BESS model.

Figure 2 shows that the output active power P^{bess} and the output reactive power Q^{bess} of BESSs need to be controlled in the circular area. Here, $P^{bess,cap}$ is the installed capacity of the BESS. The power of BESSs satisfies the following constraints [35]:

$$\left\|\begin{bmatrix}P_{i,t}^{bess}\\ Q_{i,t}^{bess}\end{bmatrix}\right\|_2\leq P_i^{bess,\max} \tag{6}$$

$$0\leq P_{i,t}^{bess,d}\leq P_i^{bess,\max} \tag{7}$$

$$-P_i^{bess,\max}\leq P_{i,t}^{bess,c}\leq 0 \tag{8}$$

where $P_{i,t}^{bess}$ and $Q_{i,t}^{bess}$ are the output active and reactive power of BESS i at time period t, respectively; $P_i^{bess,\max}$ is the maximum output active power of BESS i, which is determined by the number and rated power of the power converter in the BESS; and $P_{i,t}^{bess,d}$ and $P_{i,t}^{bess,c}$ are the discharging and charging power of BESS i at time period t, respectively.

The charging and discharging efficiencies of BESSs are considered to ensure that the energy stored in BESSs satisfies the following constraints [36].

$$0\leq E_{i,t}\leq C_i^{N} \tag{9}$$

$$E_{i,t}=E_{i,t-1}+H_{i,t}\eta_c P_{i,t}^{bess,c}-(1-H_{i,t})\frac{P_{i,t}^{bess,d}}{\eta_d} \tag{10}$$

$$E_{i,T}=E_{i,0} \tag{11}$$

$$SOC_{\min}\leq SOC_{i,t}\leq SOC_{\max} \tag{12}$$

where C_i^{N} is the rated capacity of BESS i; $E_{i,t}$ is the energy stored in BESS i at time period t, which limits the energy stored in BESS at each time period within its rated capacity; η_c and η_d are the charging and discharging efficiencies of BESSs, respectively; $H_{i,t}$ is a variable that represents the charging state ($H_{i,t}>0$) or discharging state ($H_{i,t}<0$) of BESS i; $E_{i,T}$ is the remaining energy of BESS i at the end time period; $E_{i,0}$ is the initial energy stored in BESS i at the beginning time period; $SOC_{i,t}$ is the state of charge of BESS i at time period t; and $SOC_{\min}$ and $SOC_{\max}$ are the permissible minimum and maximum states of charge, respectively.

Equation (10) establishes the power balance relationship of BESSs between adjacent time periods. Equation (11) specifies that the energy stored in the BESS should return to the initial value after a working cycle is completed.

4) Peak Load Shifting Constraints of Distribution Network

Figure 3 shows a schematic diagram of a BESS participating in the peak load shifting of a distribution network, where $P^{grid,peak}$ and $P^{grid,valley}$ are the peak and valley target power of the distribution network, respectively. The total active power interaction between the distribution network and the transmission network should satisfy (13).

$$P^{grid,valley}\leq P_t^{grid}\leq P^{grid,peak} \tag{13}$$

where P_t^{grid} is the interactive active power between the distribution network and the transmission network.

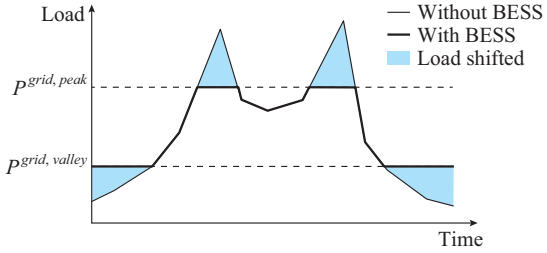

Fig. 3. Schematic diagram of a BESS participating in peak load shifting of a distribution network.

5) Transmission Capacity Constraints of Line

The upper limit constraint of the transmission capacity of line is mathematically expressed as:

$$\left\| \begin{bmatrix} P_{i,j,t}^{l} \\ Q_{i,j,t}^{l} \end{bmatrix} \right\|_2 \le S_{i,j}^{l} \tag{14}$$

where $S_{i,j}^{l}$ is the transmission capacity of line l whose starting node is i and ending node is j.

6) Voltage Constraints of System Node

The voltage constraint of the system node [16] is given by (15).

$$U_i^{\min} \le U_{i,t} \le U_i^{\max} \tag{15}$$

where $U_{i,t}$ is the voltage amplitude of node i at time period t; and $U_i^{\min}$ and $U_i^{\max}$ are the minimum and maximum voltages of node i, respectively.

7) Operation Constraints of PV Power Station

The operation constraints of PV power station are represented by (16) and (17). Although the PV power station can generate reactive power, it must satisfy the constraint given in (17).

$$0 \le P_{n,t}^{pv} \le P_{n,t}^{pv,\max} \tag{16}$$

$$\left\| \begin{bmatrix} P_{n,t}^{pv} \\ Q_{n,t}^{pv} \end{bmatrix} \right\|_2 \le S_n^{pv} \tag{17}$$

where $P_{n,t}^{pv}$ and $Q_{n,t}^{pv}$ are the active and reactive power outputs of PV power station n at time period t, respectively; $P_{n,t}^{pv,\max}$ is the maximum active power of PV power station n at time period t; and S_n^{pv} is the installed capacity of PV power station n.

8) Main Transformer Capacity and Power Factor Constraints of Distribution Network

To ensure economic viability and that the service life of the transformer is not reduced, the long-term working load rate should not exceed 85%. If the overload is frequent (if the overload time exceeds 30%), the service life of the transformer is adversely affected. In view of the characteristics of electric power generation, the power factors at the users' end have an important effect on the full utilization of the equipment, which can save electrical energy and improve voltage quality. To improve the economic benefit of the electricity supply and its consumption by users, the constraints of the main transformer capacity and the power factor of the distribution network are also established.

$$P^{grid,\min} \le P_t^{grid} \le P^{grid,\max} \tag{18}$$

$$Q^{grid,\min} \le Q_t^{grid} \le Q^{grid,\max} \tag{19}$$

$$\left\| \begin{bmatrix} P_t^{grid} \\ Q_t^{grid} \end{bmatrix} \right\|_2 \le \sum_{i=1}^{M} S_{trsf,N}^{i} \tag{20}$$

$$\frac{P_t^{grid}}{\left\| \begin{bmatrix} P_t^{grid} \\ Q_t^{grid} \end{bmatrix} \right\|_2} \ge \varphi_N \tag{21}$$

where Q_t^{grid} is the reactive interactive power of transformer i at time period t; $S_{trsf,N}^{i}$ is the rated capacity of transformer i; M is the number of connected transformers; and φ_N is the minimum power factor allowed by the total load of the distribution network.

Formulae (18) and (19) represent the constraints of the active and reactive interactive power of the transformer between the transmission network and the distribution network, respectively. Formula (20) represents the capacity constraint of the transformer between the distribution network and the transmission network. Formula (21) is the power factor constraint of the interactive power between the distribution network and the transmission network.

III. Solution of Model

To avoid the iterative solving process of the intelligent algorithm, the model is converted to an MILP problem. The model needs to be linearized first and then solved using commercial software. In this study, the big M method [15] is adopted to linearize the nonlinear variables in the model.

A. Linear Transformation of Objective Function

The objective function has a nonlinear term $|U_{i,t}-1|$, which is linearized as:

$$|U_{i,t}-1| = 2V_{i,t} - (U_{i,t}-1) \tag{22}$$

where $V_{i,t}$ is a continuous variable that satisfies the constraints in (23).

$$\begin{cases} 0 \le V_{i,t} - (U_{i,t}-1) \le M(1-\alpha_{i,t}) \\ 0 \le V_{i,t} \le M\alpha_{i,t} \end{cases} \tag{23}$$

where M is an arbitrarily large positive number; and $\alpha_{i,t}$ is a binary variable. When $U_{i,t} \ge 0$, $\alpha_{i,t}=1$, $V_{i,t}=U_{i,t}-1$, then $|U_{i,t}-1| = U_{i,t}-1$. When $U_{i,t} \le 0$, $\alpha_{i,t}=0$, $V_{i,t}=1-U_{i,t}$, then $|U_{i,t}-1| = 1-U_{i,t}$. Thus, (22) is linearized.

B. Linear Transformation of Constraints

In the power flow constraint of the distribution network containing distributed energy storage given in (4), $D_{j,i,t}^{l}(U_{j,t}-U_{i,t})$ is a nonlinear term, and the linearization transformation process is shown in (24)-(27).

$$\frac{r_{j,i}^{l}P_{j,i,t}^{l} + x_{j,i}^{l}Q_{j,i,t}^{l}}{U_0} = 2(W_{j,t}-W_{i,t}) - (U_{j,t}-U_{i,t}) \tag{24}$$

$$\begin{cases} W_{j,t} = D_{j,i,t}^{l}U_{j,t} \\ W_{i,t} = D_{j,i,t}^{l}U_{i,t} \end{cases} \tag{25}$$

$$\begin{cases} -M(1-D_{j,i,t}^{l}) \le W_{j,t} - U_{j,t} \le M(1-D_{j,i,t}^{l}) \\ -M(1-D_{j,i,t}^{l}) \le W_{i,t} - U_{i,t} \le M(1-D_{j,i,t}^{l}) \end{cases} \tag{26}$$

$$\begin{cases} 0 \le W_{j,t} \le MD_{j,i,t}^{l} \\ 0 \le W_{i,t} \le MD_{j,i,t}^{l} \end{cases} \tag{27}$$

For the nonlinear term, i.e., $P_{j,i,t}^{l}D_{j,i,t}^{l}$ in (5), the linearization transformation process is shown in (28)-(30).

$$V_{j,i,t}^{l} = P_{j,i,t}^{l}D_{j,i,t}^{l} \tag{28}$$

$$\begin{cases} V_{j,i,t}^{l} \ge 0 \\ P_{j,i,t}^{l} - V_{j,i,t}^{l} \le 0 \end{cases} \tag{29}$$

$$\begin{cases} 0 \le V^l_{j,i,t} - P^l_{j,i,t} \le M(1 - D^l_{j,i,t}) \\ 0 \le V^l_{j,i,t} \le M D^l_{j,i,t} \end{cases} \tag{30}$$

By the above derivation, when $D^l_{j,i,t} > 0$, the power flow direction is from j to i; when $D^l_{j,i,t} < 0$, the power flow direction is from i to j.

In (10), the nonlinear terms $H_{i,t}P^{bess,c}_{i,t}$ and $H_{i,t}P^{bess,d}_{i,t}$ are linearized in the same manner.

C. Model Solving Procedure

Figure 4 shows the flow chart of the model solution. Before the model is solved, the parameters of the distribution network should first be read, including the network structure, PV station parameters, and BESS parameters. Then, all the data are put into the MILP model to solve it. The MILP model includes objective functions, constraints, and their linearization process. Finally, the optimal BESS operation curve can be obtained.

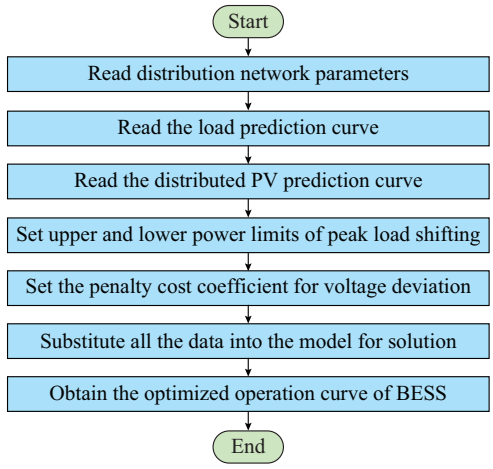

Fig. 4. Flow chart of model solution.

IV. Simulation Results and Discussion

A. Simulation Background

In this study, a modified IEEE 33-node distribution system is used to simulate and verify the model. The system consists of 33 nodes and 32 branches. CPLEX is used to solve the model. The topology of the modified IEEE 33-node system is shown in Fig. 5.

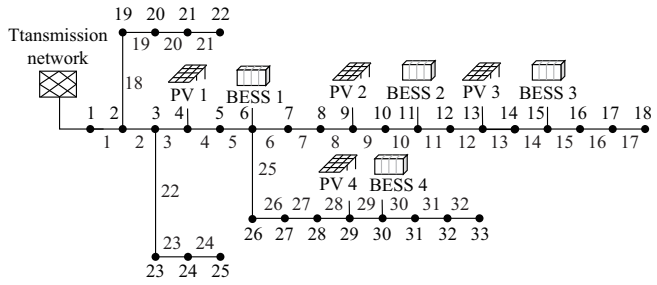

Fig. 5. Modified IEEE 33-node system.

Four PV stations (PV 1-4) and four BESSs (BESS 1-4) are connected to the system, and the parameters are presented in Table I. The battery type of the BESS is a lithium iron phosphate battery and the capacity of each BESS is 2 MWh. The power prediction curves of the PV stations are shown in Fig. 6. The branch parameters and the maximum static load of the modified IEEE 33-node system are presented in Tables II and III, respectively. The time-of-use electricity price of commercial load in Shanghai, China, in summer is adopted in the simulation (see Table IV for details). The time period is set to be 15 min. Therefore, a day is divided into 96 time periods. Only unidirectional power flow is allowed in the simulation owing to the radial network architecture of this system.

TABLE I
Parameters of PV Station and BESS

Station	Node	Installed capacity (MW)
PV 1	4	2.0
PV 2	9	2.5
PV 3	13	2.0
PV 4	29	2.5
BESS 1	6	1.0
BESS 2	11	1.0
BESS 3	15	1.0
BESS 4	30	1.0

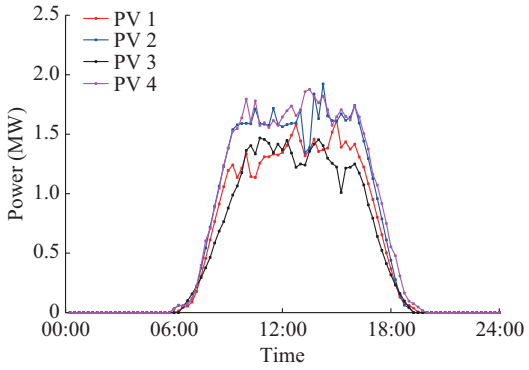

Fig. 6. Power prediction curves of PV 1-4.

B. Simulation Results and Discussion Without BESS

The power curves of system operation and the node voltage profile without BESSs are shown in Figs. 7 and 8, respectively. In terms of the DG, the peak load period is reduced to some extent because of the role of the distributed PV station during daytime. However, PV power curtailment occurs at the PV stations to some extent at a rate of approximately 6.34% owing to the power limit of the transmission line. During the peak-load period at night, the peak load hardly varies because of the absence of PV power output. In terms of the system node voltage, the allowable deviation of a three-phase power supply voltage of 10 kV (or less) is ±7% of the rated voltage according to the Chinese national standard GB/T 12325-2008. Figure 8 shows that the overall voltage deviation of the distribution network is high without BESS, and the minimum voltage drops to approximately 0.86 p.u. at approximately 07:30 p.m. because of the long supply radius. The voltage deviation is approximately 14%.

TABLE II
BRANCH PARAMETERS OF MODIFIED IEEE 33-NODE SYSTEM

Branch No.	Beginning node	End node	Impedance (p.u.)	Transmission capacity (MW)	Branch No.	Beginning node	End node	Impedance (p.u.)	Transmission capacity (MW)
1	1	2	0.0922+j0.4070	13.5	17	17	18	0.7320+j0.5740	3.5
2	2	3	0.4930+j0.2511	13.5	18	2	19	0.1640+j0.1565	3.5
3	3	4	0.3660+j0.1864	13.5	19	19	20	1.5042+j1.3554	3.5
4	4	5	0.3811+j0.1941	13.5	20	20	21	0.4095+j0.4784	3.5
5	5	6	0.8190+j0.7070	13.5	21	21	22	0.7089+j0.9373	3.5
6	6	7	0.1872+j0.6188	5.5	22	3	23	0.4512+j0.3083	3.5
7	7	8	0.7144+j0.2351	5.5	23	23	24	0.8980+j0.7091	3.5
8	8	9	1.0300+j0.7400	5.5	24	24	25	0.8960+j0.7011	3.5
9	9	10	1.0440+j0.7400	5.5	25	6	26	0.2030+j0.1034	3.5
10	10	11	0.1966+j0.0650	5.5	26	26	27	0.2842+j0.1447	3.5
11	11	12	0.3744+j0.7400	3.5	27	27	28	1.0590+j0.9337	3.5
12	12	13	1.4680+j1.1550	3.5	28	28	29	0.8042+j0.7006	3.5
13	13	14	0.5416+j0.7129	3.5	29	29	30	0.5075+j0.2585	3.5
14	14	15	0.5910+j0.5260	3.5	30	30	31	0.9744+j0.9630	3.5
15	15	16	0.7463+j0.5450	3.5	31	31	32	0.3105+j0.3619	3.5
16	16	17	1.2890+j1.7210	3.5	32	32	33	0.3410+j0.5362	3.5

TABLE III
MAXIMUM STATIC LOAD OF MODIFIED IEEE 33-NODE SYSTEM

Node	Load (MW)	Node	Load (MW)
1	0+j0	18	0.09+j0.040
2	0.100+j0.040	19	0.09+j0.040
3	0.090+j0.040	20	0.09+j0.040
4	0.120+j0.030	21	0.09+j0.040
5	0.060+j0.020	22	0.09+j0.040
6	0.060+j0.020	23	0.09+j0.030
7	0.100+j0.030	24	0.20+j0.080
8	0.100+j0.030	25	0.20+j0.080
9	0.060+j0.020	26	0.06+j0.025
10	0.060+j0.020	27	0.06+j0.025
11	0.045+j0.015	28	0.06+j0.020
12	0.060+j0.025	29	0.12+j0.030
13	0.060+j0.025	30	0.20+j0.080
14	0.120+j0.050	31	0.15+j0.060
15	0.060+j0.010	32	0.21+j0.080
16	0.060+j0.025	33	0.06+j0.020
17	0.060+j0.020		

TABLE IV
TIME-OF-USE ELECTRICITY PRICE

Time	Electricity price (¥/kWh)
Peak time (08:00-11:00, 13:00-15:00, 18:00-21:00)	1.196
Usual time (06:00-08:00, 11:00-13:00, 15:00-18:00, 21:00-22:00)	0.742
Valley time (22:00-06:00)	0.353

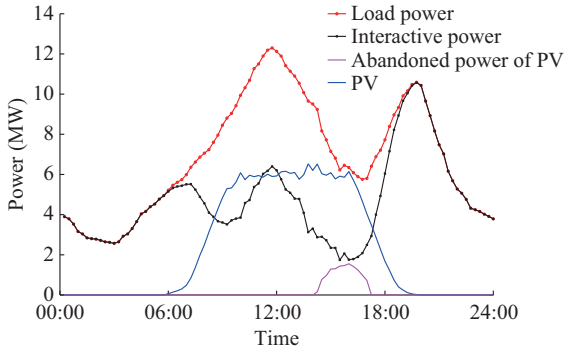

Fig. 7. Power curves of system operation without BESSs.

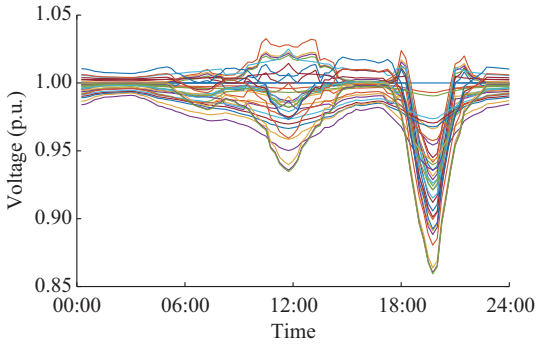

Fig. 8. Voltage profiles of nodes without BESSs.

C. Simulation Results and Discussion with BESS

After the BESS is connected to the distribution network, $P^{grid,peak}$ and $P^{grid,valley}$ are set to be 7.39 and 3.17 MW, respectively, and the BESS charging and discharging efficiencies are 0.95.

1) Analysis of System Operation

The power curves of system operation with BESSs are

shown in Fig. 9. It can be seen that after the BESSs are connected, the interactive power between the system and the transmission network is significantly reduced, and no case higher than $P^{grid,peak}$ or lower than $P^{grid,valley}$ occurs. At the same time, the problem of abandoned power is significantly improved after the connection of BESSs.

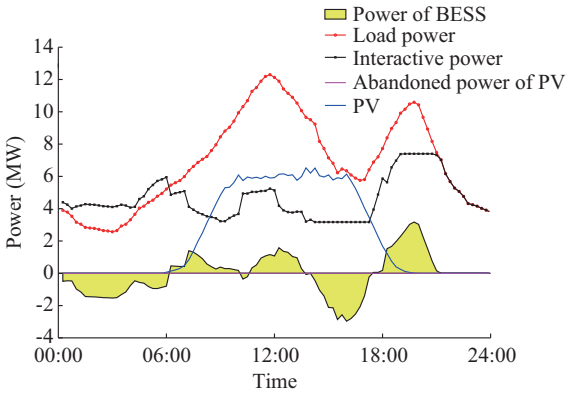

Fig. 9. Power curves of system operation with BESSs.

2) Analysis of Distributed Energy Storage Operation and Effect of Voltage Regulation

Figure 10 shows the power variations of each BESS in a day. The BESS needs to perform the peak load shifting task. Thus, the active power variation trends of the four BESSs are essentially the same, whereas the reactive power variation exhibits different characteristics. BESS 1 is installed at the junction of the branches 6-18 and 6-33. These two branches present the most prominent low-voltage problem. The BESSs can provide overall support of active and reactive power for the two branches. The power variation diagram shows that BESS 1 provides more reactive power during the night, whereas the reactive power provided during the daytime varies significantly. Reactive power absorption occurs more in the morning and less in the afternoon. This indicates that there is a certain redundancy of reactive power near node 6 during daytime, thus the node voltage is high. In addition, since BESS 2 is installed between PV 2 and PV 3, and the PV stations around are relatively dense, it absorbs more reactive power. Therefore, the transmission power of the branches is limited, and there is excess reactive power around node 11. BESS 3 can focus on the low-voltage problem of nodes 15-18, whereas BESS 4 focuses on the low-voltage problem between nodes 30 and 33. The two BESSs provide reactive power throughout the day, which indicates that the reactive power deficiencies of nodes 15-18 and 30-33 are relatively large. However, during the peak hours of the night load, the reactive power provided by BESS 4 decreases to a certain extent because BESS 4 needs to provide active power to perform the task of peak load shifting. Thus, the reactive power output is limited to a certain extent.

Figure 11 shows the voltage distribution of the system nodes with BESSs. Under the regulation of the BESSs, the low-voltage problem of the system during the peak period of night load is solved. The minimum voltage increases from 0.86 to 0.955 p.u.. In addition, the voltage levels in other time periods improve to different degrees, maintaining the system voltage deviation within ±5% in a day.

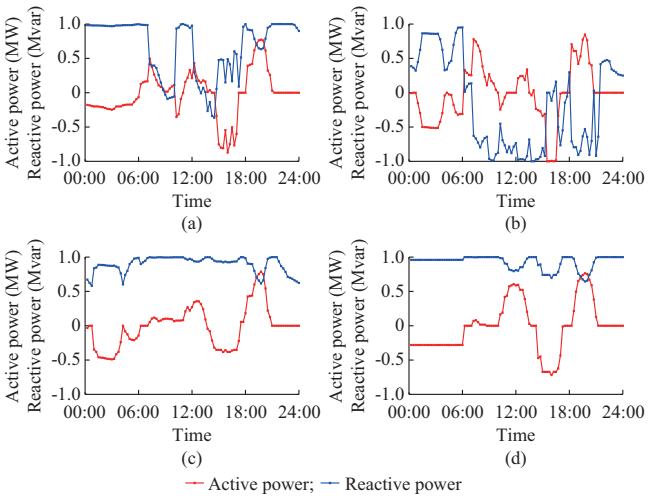

Fig. 10. Power diagram of BESS 1-4. (a) BESS 1. (b) BESS 2. (c) BESS 3. (d) BESS 4.

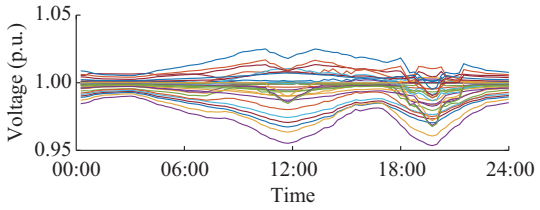

Fig. 11. Node voltage distribution of systems nodes with BESSs.

In this study, 10:30 a.m. and 07:45 a.m. are selected as typical time when the system has no access to energy storage to investigate the improvement of the system node voltage with and without BESSs. The node voltage distribution diagram at the typical time is shown in Fig. 12.

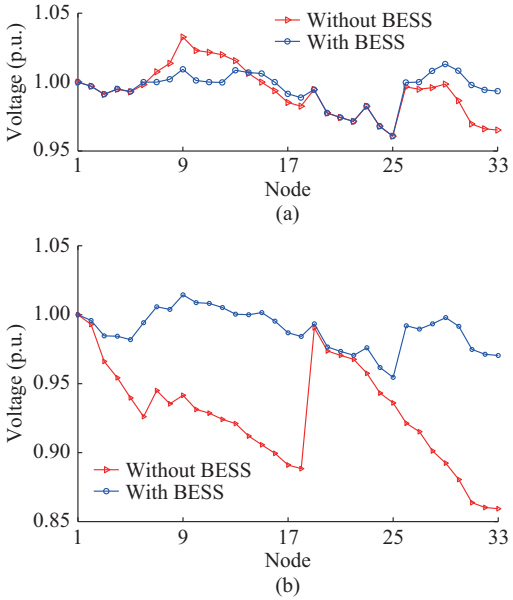

Fig. 12. Node voltage distribution at typical time. (a) 10:30 a.m.. (b) 07:45 a.m..

Figure 12 shows that the voltage deviation near node 9 decreases to a certain extent at 10:30 a.m.. The problem of

high voltage in the system improves to some extent. The time with the lowest voltage (07:45 a.m.) is one of the most prominent time with respect to the low-voltage problems in the system, particularly at nodes 7-18 and nodes 26-33. After the BESSs are connected, the voltage of each node increases significantly, and the voltage deviation is controlled within the allowable range.

After the BESSs are connected, the voltage qualification rate of the system increases from 94.73% to 100%. The maximum and minimum voltage deviations of the system decrease significantly. The maximum voltage deviation decreases from 3.27% to 2.51%. The minimum voltage deviation decreases from 14.06% to 4.54%. The average voltage deviation of the system decreases from 1.30% to 0.66%. Therefore, after the BESSs are connected, the low-voltage problem in the system is effectively solved, and the voltage level improves significantly.

3) Analysis of Peak Load Shifting of Distributed Energy Storage

After BESSs are connected, the maximum interactive power between the system and the transmission network decreases from 10.57 to 7.40 MW, reducing the peak load by approximately 30%. The valley period of system is at a period with a small load at night and the peak period of the PV station during daytime. The minimum interactive power between the system and the transmission network increases from 1.74 to 3.17 MW. The maximum peak-valley difference of the system decreases from 8.83 to 4.23 MW. Therefore, the BESS plays an important role in peak load shifting. The cost of interactive power decreases from ¥90483 to ¥81866.

V. Conclusion

An optimal dispatch method for distributed energy storage considering peak load shifting and renewable energy integration is presented in the paper. The system power flow calculation and energy storage optimization dispatch are transformed into MILP problems, thus the use of a complex optimization algorithm is avoided, which significantly improves the accuracy of the model. Finally, the proposed model and solution technique are validated using the modified IEEE 33-node system. The conclusions are drawn as follows.

1) The BESS has a four-quadrant regulating capacity, which can participate in the voltage regulation of the distribution network and significantly improve the system voltage level. For the IEEE 33-node system, which is a typical example of a distribution network, the maximum voltage deviation can be reduced from 14.06% to 4.54%, and the voltage qualification rate can be significantly improved.

2) The BESS plays an important role in peak load shifting. The interactive power between the distribution network and the transmission network can be limited in a certain range using the proposed MILP model, thereby significantly reducing the peak consumption.

3) The BESS can promote the absorption of distributed PV power and improve the efficiency of renewable energy. In this study, the total PV power abandoned in the distribution network can be reduced from 6.34% to 0%.

The proposed BESS dispatch model is mainly used for the voltage regulation of distribution network and the optimization of peak-load days. The above results fully verify the validity of the model. However, in this study, the line capacity, main transformer capacity, power factor, and other factors are considered as constraints in the model without in-depth analysis. This is planned as future research.

References

[1] X. Li, D. Hui, and X. Lai, "Battery energy storage station (BESS)-based smoothing control of photovoltaic (PV) and wind power generation fluctuations," *IEEE Transactions on Sustainable Energy*, vol. 4, no. 2, pp. 464-473, Apr. 2013.

[2] Y. Li, H. Zhang, X. Liang *et al*., "Event-triggered-based distributed cooperative energy management for multi-energy systems," *IEEE Transactions on Industrial Informatics*, vol. 15, no. 4, pp. 2008-2022, Apr. 2019.

[3] R. Li, W. Wang, and M. Xia, "Cooperative planning of active distribution system with renewable energy sources and energy storage systems," *IEEE Access*, vol. 6, pp. 5916-5926, Dec. 2017.

[4] D. Zarrilli, A. Giannitrapani, S. Paoletti *et al*., "Energy storage operation for voltage control in distribution networks: a receding horizon approach," *IEEE Transactions on Control Systems Technology*, vol. 26, no. 3, pp. 599-609, Mar. 2018.

[5] Z. Wang, H. Lin, and Y. Ma, "A control strategy of modular multilevel converter with integrated battery energy storage system based on battery side capacitor voltage control," *Energies*, vol. 12, no. 11, pp. 2151-2170, Jun. 2019.

[6] J. Zhao and B. Shen, "The strategies for improving energy efficiency of power system with increasing share of wind power in China," *Energies*, vol. 12, no. pp. 2376-2397, Jun. 2019.

[7] D. Zhu, W. Liu, Y. Hu *et al*., "A practical load-source coordinative method for further reducing curtailed wind power in China with energy-intensive loads," *Energies*, vol. 11, no. 11, pp. 2925-2938, Oct. 2018.

[8] M. Ndawula, S. Djokic, and I. Hernando-Gil, "Reliability enhancement in power networks under uncertainty from distributed energy resources," *Energies*, vol. 12, no. 3, pp. 531-554, Feb. 2019.

[9] S. Lakshminarayana, Y. Xu, H. Poor *et al*., "Cooperation of storage operation in a power network with renewable generation," *IEEE Transactions on Smart Grid*, vol. 7, no. 4, pp. 2108-2122, Jul. 2016.

[10] A. Azizivahed, M. Barani, S. Razavi *et al*., "Energy storage management strategy in distribution networks utilised by photovoltaic resources," *IET Generation, Transmission & Distribution*, vol. 12, no. 21, pp. 5627-5638, Nov. 2018.

[11] A. Davda, B. Azzopardi, B. Parekh *et al*., "Dispersed generation enable loss reduction and voltage profile improvement in distribution network–case study, Gujarat, India," *IEEE Transactions on Power Systems*, vol. 29, no. 3, pp. 1242-1249, May 2014.

[12] C. Zhang, H. Chen, Z. Liang *et al*., "Interval voltage control method for transmission systems considering interval uncertainties of renewable power generation and load demand," *IET Generation, Transmission & Distribution*, vol. 12, no. 17, pp. 4016-4025, Sept. 2018.

[13] A. Bokhari, A. Raza, M. Diaz-Aguiló *et al*., "Combined effect of CVR and DG penetration in the voltage profile of low-voltage secondary distribution networks," *IEEE Transactions on Power Delivery*, vol. 31, no. 1, pp. 286-293, Feb. 2016.

[14] N. Meena, S. Parashar, A. Swarnkar *et al*., "Improved elephant herding optimization for multiobjective DER accommodation in distribution systems," *IEEE Transactions on Industrial Informatics*, vol. 14, no. 3, pp. 1029-1039, Mar. 2018.

[15] X. Li, Y. Huang, and S. Yang. "Demand response measures and its quantitative effects in promoting renewable energy accommodation in high proportional renewable energy scenario," *The Journal of Engineering*, vol. 13, pp. 1367-1372, Oct. 2017.

[16] B. Zeng, J. Zhang, X. Yang *et al*., "Integrated planning for transition to low-carbon distribution system with renewable energy generation and demand response," *IEEE Transactions on Power Systems*, vol. 29, no. 3, pp. 1153-1165, May 2014.

[17] H. Zhang, Y. Li, D. W. Gao *et al*., "Distributed optimal energy management for energy internet," *IEEE Transactions on Industrial Informatics*, vol. 13, no. 6, pp. 3081-3097, Dec. 2017.

[18] M. Asensio, P. M. de Quevedo, G. Muñoz-Delgado *et al*., "Joint distri-

bution network and renewable energy expansion planning considering demand response and energy storage–Part I: stochastic programming model," *IEEE Transactions on Smart Grid*, vol. 9, no. 2, pp. 655-666, Mar. 2018.

[19] M. Asensio, P. M. de Quevedo, G. Muñoz-Delgado *et al*., "Joint distribution network and renewable energy expansion planning considering demand response and energy storage–Part II: numerical results," *IEEE Transactions on Smart Grid*, vol. 9, no. 2, pp. 667-675, Mar. 2018.

[20] P. M. de Quevedo, G. Muñoz-Delgado, and J. Contreras, "Impact of electric vehicles on the expansion planning of distribution systems considering renewable energy, storage, and charging stations," *IEEE Transactions on Smart Grid*, vol. 10, no. 1, pp. 794-804, Jan. 2019.

[21] M. Zidar, P. S. Georgilakis, N. D. Hatziargyriou *et al*., "Review of energy storage allocation in power distribution networks: applications, methods and future research," *IET Generation, Transmission & Distribution*, vol. 10, no. 3, pp. 645-652, Feb. 2016.

[22] X. Li and S. Wang. "A review on energy management, operation control and application methods for grid battery energy storage systems," *CSEE Journal of Power and Energy Systems*, vol. 7, no. 5, pp. 1026-1040, Sept. 2021.

[23] X. Shen, M. Shahidehpour, Y. Han *et al*., "Expansion planning of active distribution networks with centralized and distributed energy storage systems," *IEEE Transactions on Sustainable Energy*, vol. 8, no. 1, pp. 126-134, Jan. 2017.

[24] A. W. Bizuayehu, A. A. S. de la Nieta, J. Contreras *et al*., "Impacts of stochastic wind power and storage participation on economic dispatch in distribution systems," *IEEE Transactions on Sustainable Energy*, vol. 7, no. 3, pp. 1336-1345, Jul. 2016.

[25] Y. Zhang, S. Ren, Z. Dong *et al*., "Optimal placement of battery energy storage in distribution networks considering conservation voltage reduction and stochastic load composition," *IET Generation, Transmission & Distribution*, vol. 11, no. 15, pp. 3862-3870, Oct. 2017.

[26] W. Gan, X. Ai, J. Fang *et al*., "Security constrained co-planning of transmission expansion and energy storage," *Applied Energy*, vol. 239, pp. 383-394, Apr. 2019.

[27] Y. Wang, K. Tan, X. Peng *et al*., "Coordinated control of distributed energy-storage systems for voltage regulation in distribution networks," *IEEE Transactions on Power Delivery*, vol. 31, no. 3, pp. 1132-1141, Jun. 2016.

[28] A. Giannitrapani, S. Paoletti, A. Vicino *et al*., "Optimal allocation of energy storage systems for voltage control in LV distribution networks," *IEEE Transactions on Smart Grid*, vol. 8, no. 6, pp. 2859-2870, Nov. 2017.

[29] D. Zarrilli, A. Giannitrapani, S. Paoletti *et al*., "Energy storage operation for voltage control in distribution networks: a receding horizon approach," *IEEE Transactions on Control Systems Technology*, vol. 26, no. 2, pp. 599-609, Mar. 2018.

[30] H. Sugihara, K. Yokoyama, O. Saeki *et al*., "Economic and efficient voltage management using customer-owned energy storage systems in a distribution network with high penetration of photovoltaic systems," *IEEE Transactions on Power Systems*, vol. 28, no. 1, pp. 102-111, Feb. 2013.

[31] L. Wang, D. Liang, A. Crossland *et al*., "Coordination of multiple energy storage units in a low-voltage distribution network," *IEEE Transactions on Smart Grid*, vol. 6, no. 6, pp. 2906-2918, Nov. 2015.

[32] S. Sami, M. Cheng, J. Wu *et al*., "A virtual energy storage system for voltage control of distribution networks," *CSEE Journal of Power and Energy Systems*, vol. 4, no. 2, pp. 146-154, Jun. 2018.

[33] G. Chang, S. Chu, and H. Wang, "An improved backward/forward sweep load flow algorithm for radial distribution systems," *IEEE Transactions on Power Systems*, vol. 22, no. 2, pp. 882-884, May 2007.

[34] J. Teng and C. Chang. "Backward/forward sweep-based harmonic analysis method for distribution systems," *IEEE Transactions on Power Delivery*, vol. 22, no. 3, pp. 1665-1672, Jul. 2007.

[35] T. Nguyen, M. Crow, and A. Elmore. "Optimal sizing of a vanadium redox battery system for microgrid systems," *IEEE Transactions on Sustainable Energy*, vol. 6, no. 3, pp. 729-737, Jul. 2015.

[36] J. Lei, Q. Gong, J. Liu *et al*., "Optimal allocation of a VRB energy storage system for wind power applications considering the dynamic efficiency and life of VRB in active distribution networks," *IET Renewable Power Generation*, vol. 13, no. 4, pp. 563-571, Mar. 2019.

Xiangjun Li received the B. E. degree in electrical engineering from Shenyang University of Technology, Shenyang, China, in July 2001, and the M.E. and Ph.D. degrees in electrical and electronic engineering from Kitami Institute of Technology (KIT), Kitami, Japan, in 2004 and 2006, respectively. From May 2006 to March 2010, he worked as a Postdoctoral Research Fellow at Korea Institute of Energy Research (KIER), Daejeon, Korea, and Tsinghua University, Beijing, China, respectively. In March 2010, he joined the Energy Storage and Electrical Engineering Department (ESED) (formerly: Electrical Engineering and New Material Department), China Electric Power Research Institute (CEPRI), Beijing, China. His research interests include large-scale energy storage technology, new energy and distributed generation, and power system operation and control.

Rui Ma received the B.E. degree from Liren College of Yanshan University, Qinhuangdao, China. Currently, he is pursuing the M.S. degree in power system and automation from China Electrical Power Research Institute (CEPRI), Beijing, China. His research interests include scheduling and control of energy storage system.

Wei Gan received the B.S. degree in electrical engineering from Huazhong University of Science and Technology (HUST), Wuhan, China, in 2016. He is currently working toward the Ph. D. degree with HUST. From 2019 to 2020, he was a visiting Ph.D. student with the Robert W. Galvin Center for Electricity Innovation, Illinois Institute of Technology, Chicago, USA. His research interests include energy storage planning, and electrified transportation operation and planning.

Shijie Yan received the B.S., M.S., and Ph.D. degrees in power electronics and drives from the School of Information Science and Engineering, Northeastern University, Shenyang, China, in 1986, 1999 and 2010, respectively. He is currently an Associate Professor with Department of Electrical Engineering, Northeastern University. His research interests include large-scale energy storage technology, power electronics, new energy generation, and electric drives.